JOINT INSTITUTE FOR NUCLEAR RESEARCH
Frank Laboratory of Neutron Physics

FINAL REPORT
ON STAGE 1 OF THE INTERNATIONAL STUDENT PRACTICE

"Coexistence of superconductivity and ferromagnetism at low-dimensional heterostructures"

Supervisor:
Dr. V. Zhaketov

Student(s):

Zaky Abdelslam Zaky Ebrahim
(Beni-Suef University)

Maha Magdy Mohamed Abdalla
(Cairo University)

Participation period:
01-24 March

Dubna, 2022

Coexistence of superconductivity and ferromagnetism at low-dimensional heterostructures

Abstract

In this study, the interaction between neutron waves and superconductor/ ferromagnetic heterostructures will be investigated. The proposed structure is Al_2O_3 / Nb(100nm) / Gd(3nm) / V(70nm) / Nb(15nm). Spin asymmetry and reflectivity are studied for both experimental data and theoretical models. By increasing the grazing angle with and without magnetization, reflectivity spectra are red shifted to higher wavelengths at optimum conditions of thicknesses and angle. Besides, the reflectivity of neutrons at different types of magnetizations (collinear and non-collinear) are reported. Then, we study the effect of changing the ferromagnetic layer (Gd) layer thickness. Besides, different ferromagnetic layers of Fe, Co, Ni and Dy are used rather than Gd. Finally, we make a comparative study between experimental X-Ray reflectivity of the structure, and we use a theoretical model to fit it.

Introduction

Ferromagnetism and superconductivity have opposite behavior and need special conditions to coexist in uniform materials because superconductors expel magnetic field according to Meissner effect, while field lines are concentrated in ferromagnetic materials according to the magnetic induction effect [1-3]. Recently, the coexistence of superconductivity and ferromagnetism heterostructures have attracted attention since the discovery of high-Tc superconducts [4-6]. Ginzburg explained the suppression of ferromagnetism via superconductivity structure in transition metals where the magnetic induction in these metals is higher than the critical field [1]. Due to the exchange interaction between ferromagnetism and superconductivity, electron spins of cooper pairs tend to be aligned in the same direction. The state of superconductivity is destroyed when the coupling energy of the electrons is lower than the Zeeman energy of a Cooper pair in an exchange field.

Artificial multilayers of ferromagnetic and superconductor materials have caught attention because of the diversity of proximity effects. These effects demonstrate how ferromagnetism and superconductivity affect each other at the S/F heterostructures' interface [4]. Proximity effect is produced at the interface between a normal metal and superconductor layer because the superconducting order parameter appears in the normal metal at a distance (coherence length, ξ) from the interface. The inverse or magnetic proximity effect describes the emergence of the magnetic order parameter in a superconductor close to the SC/FM interface [7]. At temperatures lower than the superconducting transition temperature (T_C), the proximity effect is manifested clearly. While the induced magnetism gradually vanishes when the temperature rises to T_C [7].

Magnetometers of various sorts often produce just average magnetization values. The vector magnetization is shown with exceptional spatial detail well beneath the surface using polarized neutron reflectometry (PNR) and magnetic X-ray scattering. Because neutrons have magnetic moments and can be acquired with such a wavelength comparable to lattice spacing, they are sensitive to atomic magnetic moments [8]. X-ray (XRR) and neutron reflectometry, unlike electron and optical microscopy, do not directly produce real-space images of the objects of interest. Because X-ray and neutron wavelengths are comparable to the dimensions of the sample under study, the information about the composition of the sample and its shape that appeared in the reflected spectra, including the vector magnetization depth profile, mathematical analysis must be used to extract them [8].

Results and discussions

The proposed structure is consisting of gadolinium ferromagnetic layer (Gd) sandwiched between two superconducting materials of niobium (Nb) and vanadium (V). These layers are deposited on sapphire substrate. The structure is capped with Nb layer to prevent oxidation or any undesired damaging effect. Polarized neutron reflectometry (PNR) technique will be used to study the magnetization of the sample as clear in Fig. 1. This technique is based on the interaction between the magnetic moments of the sample and magnetic momentum of the incident neutrons. As initial conditions, neutrons fall on the sample with grazing angle 7.6 mrad.

Table 1: Initial conditions of materials.

Material	Thickness nm	Magnetization Oe	Scattering length density /$Å^2$* 10^{-6}	Comment
Al_2O_3	600000	0	3.989	Substrate
Nb	80+10	260	3.919	Superconductor
Gd	3.5 nm	2000	Function	Ferromagnetic
Fe	~	~	8.024	Ferromagnetic
Co	~	~	2.265	Ferromagnetic
Ni	~	~	9.408	Ferromagnetic
Dy	~	~	5.356	Ferromagnetic
V	10 +60	200	-0.320	Superconductor

Nb	15	0	3.919	Cap layer

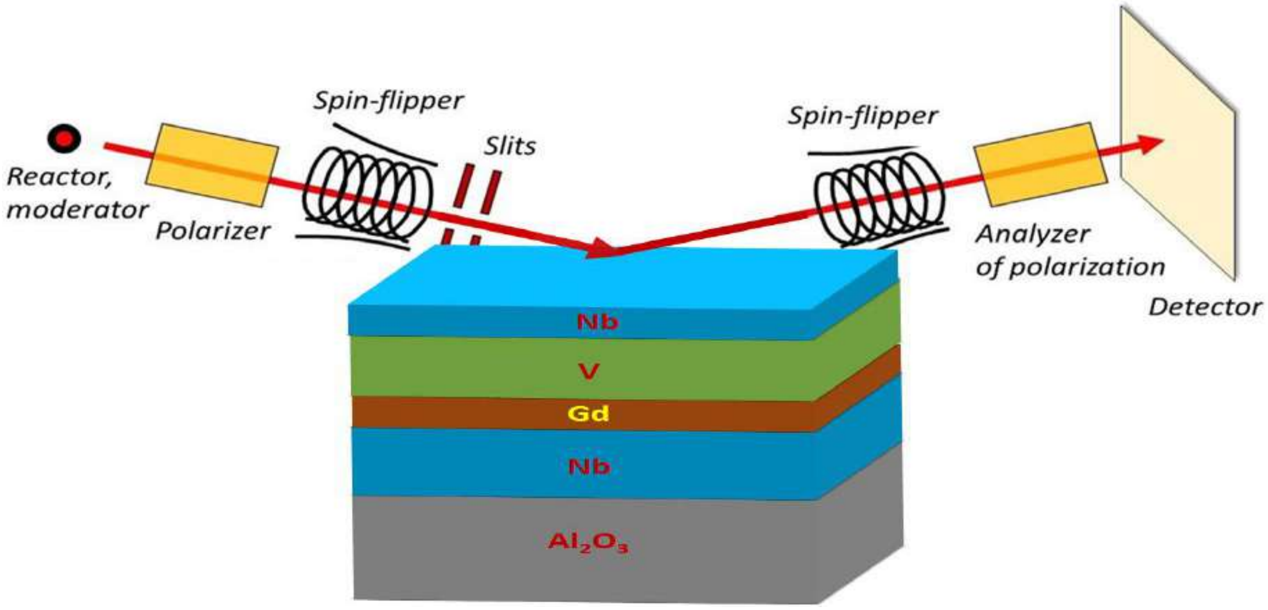

Fig.1. Schematic of PNR experiment setup and sample with deposited layers.

Figure 2 clears the effect of different parameters such as grazing angle, magnetization of V layer, magnetization of Gd layer, magnetization of Nb layer, thickness of V layer, thickness of Gd layer, and thickness of Nb layer to select the optimum conditions that make the simulated data very close to the experimental neutron spin asymmetry. As clear in Fig. 2(A), the simulated neutron spin asymmetry spectrum is very close to the experimental spectrum at angle 5.32 mrad. By increasing the grazing angle from 5.32 mrad to 9.88 mrad, the peaks and dips of the simulated spectra become larger than the experimental data. So, angle of 5.32 will be used in the following studies. In Figs. 2(B), (C), and (D), by changing the optimum magnetizations of vanadium, gadolinium, and niobium layers are 200 Oe, 1400 Oe, and 260 Oe, respectively. Also, the optimum thicknesses of vanadium, gadolinium, and niobium layers than recorded simulated neutron spin asymmetry spectra slightly similar to the experimental results are d_V = 55 nm/10 nm, d_{Gd} = 2 nm and d_{Nb} = 90 nm/ 10nm as clear in Figs. 2(E), (F), and (G), respectively. According to Table 1, thickness of superconducting materials (Nb and V) is divided in two parts with different magnetizations. A long certain distance from the interface between the ferromagnetic and superconducting materials, the super conducting material will have magnetization due to the magnetic exchange effect (proximity effect). But the residual thickness of superconductor has no magnetization.

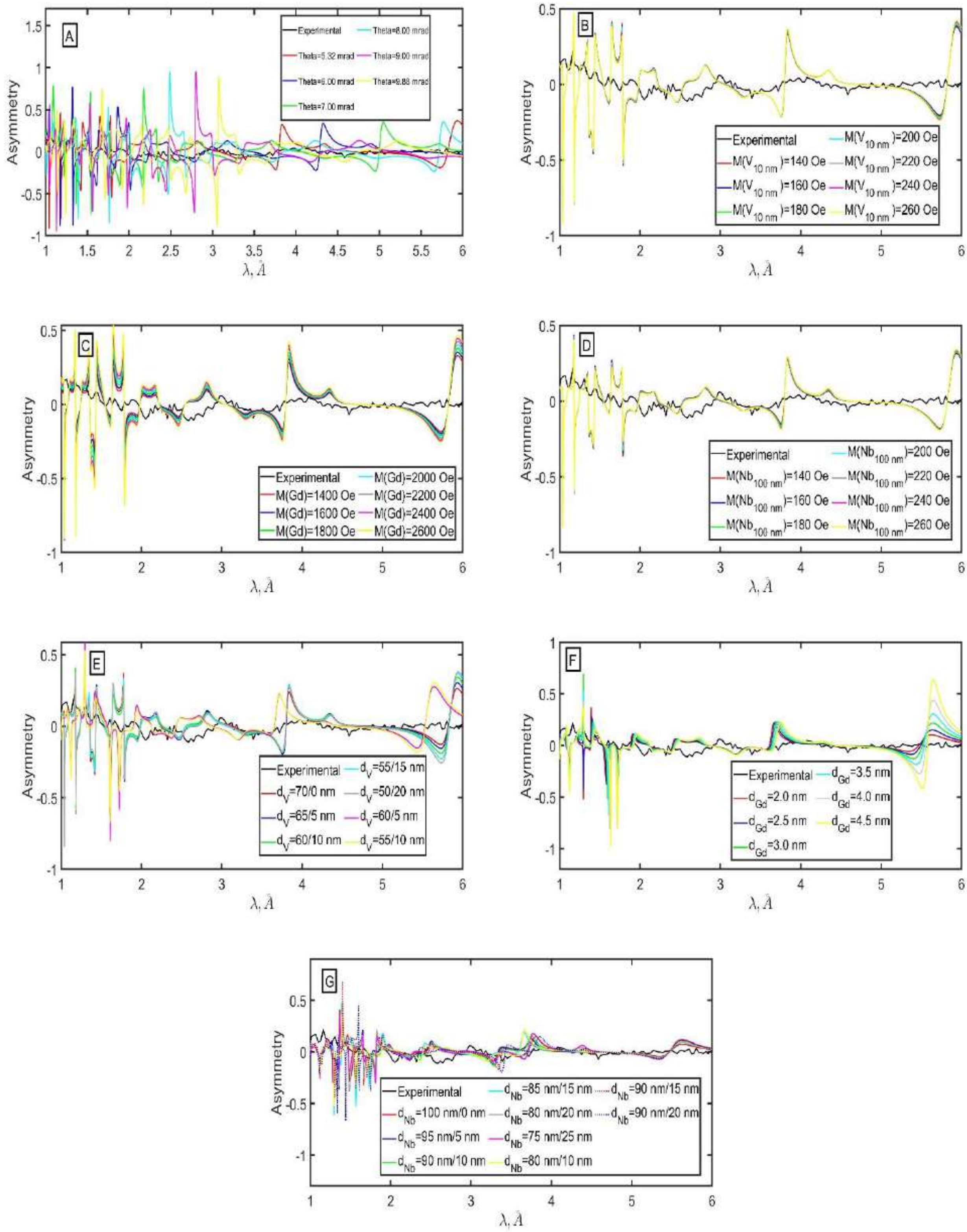

Fig. 2: The effect of (A) grazing angle, (B) magnetization of V layer, (C) magnetization of Gd layer, (D) magnetization of Nb layer, (E) thickness of V layer, (F) thickness of Gd layer, (G) thickness of Nb layer on neutron spin asymmetry.

We found that by increasing the grazing angle from 5.32 mrad to 6.32 mrad, some peaks of the simulated spectrum coincide with experimental spectrum. So, angle of 6.32 mrad will be used as optimum angle. The experimental and simulated neutron spin asymmetry at the selected condition after the above fitting process are plotted in Fig. 3. To check the quality of the fitted data, chi-squared (χ^2) will be calculated according to the following equation:

$$\chi^2 = \sum_\lambda log\left(SA_{exp} - SA_{th}\right), \tag{1}$$

where SA_{exp} and SA_{th} are experimental and theoretical neutron spin asymmetry. Before fitting processes, χ^2 was -599.7. After fitting and selecting the optimum conditions, the quality of the fitted data was enhanced and the value of χ^2 decreased to -653.2.

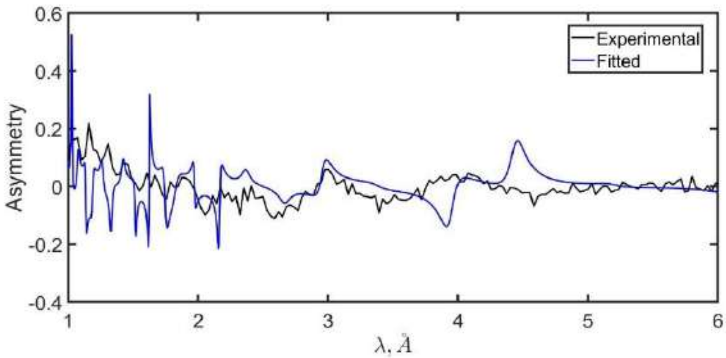

Fig. 3: The experimental (black) and fitted data (blue) of neutron spin asymmetry at the optimum conditions

Reflectivities at different angles with and without magnetization for the given structure are shown in Fig. 4. In Fig. 4(A), in case of zero magnetization, increasing the grazing angle (θ) leads to shifting of the curves to higher values of wavelength and this is according to the relation:

$$Q_z = \frac{4\pi}{\lambda}\theta. \tag{2}$$

We observe that when magnetization is equal to zero, R++ and R-- coincide with each other for all values of θ. Similar behavior of reflectivities appears in Fig. 4(B) for the nonzero magnetization case except for a slight difference in R++ and R-- is revealed at certain magnitudes of wavelengths. This small difference resulted from rising the number of spin-up neutrons reflected from the sample due to the existence of magnetization.

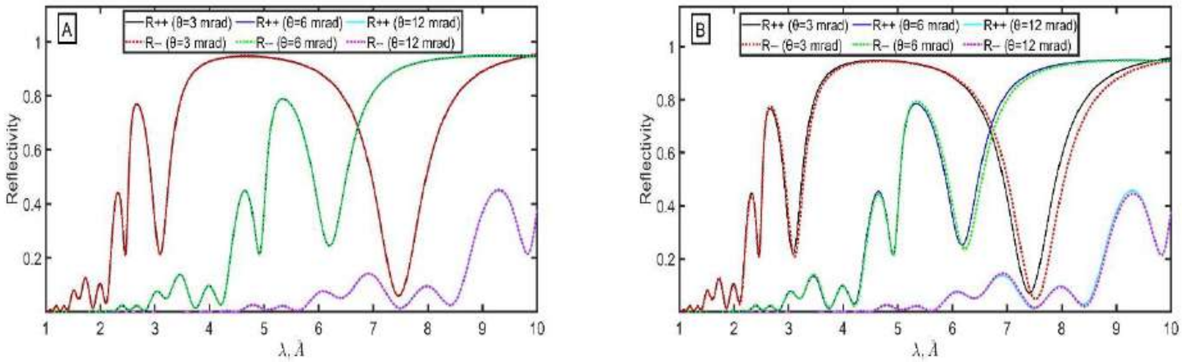

Fig. 4: Neutron reflectivity at different grazing angles (A) M=0, (B) M$\neq$ 0.

Fig. 5 displays reflectivities at different magnetizations of Gd layer for both collinear and non-collinear cases. Fig. 5(A) represents reflectivities in the case of collinear magnetization when spin flippers (SFs) are both off (R++) and both on (R--), while Fig. 5(B) represents reflectivities when SFs are the first is on and the second is off (R-+) and when the first is off and the second is on(R+-). In Fig. 5(A), it is obvious that at $M_z = 100\ Oe$ and $M_z = 1000\ Oe$, R++ and R-- almost coincide with each other, but when M became equals to 10000 Oe, a shift in R++ and R-- took place indicating that some spin down neutrons are transformed into spin up neutrons. In Fig. 5(B), we see that R-+ and R+- are equal to zeros for all values of M_z. This happens because the neutrons, which reflect from the sample, are spin down and the analyzer of polarization is designed to allow only spin up neutrons. Fig. 5(C) manifests reflectivities of non-collinear magnetization at different values of M_x of Gd layer. The inset expresses the region encircled. It is shown that there is a difference between R++ and R-- for all magnitudes of M_x. Increasing the magnetization in x-direction causes the reflectivities (R++ and R--) to decrease which can be explained by increasing the absorption of neutrons. This is plain in Fig. 5(D).

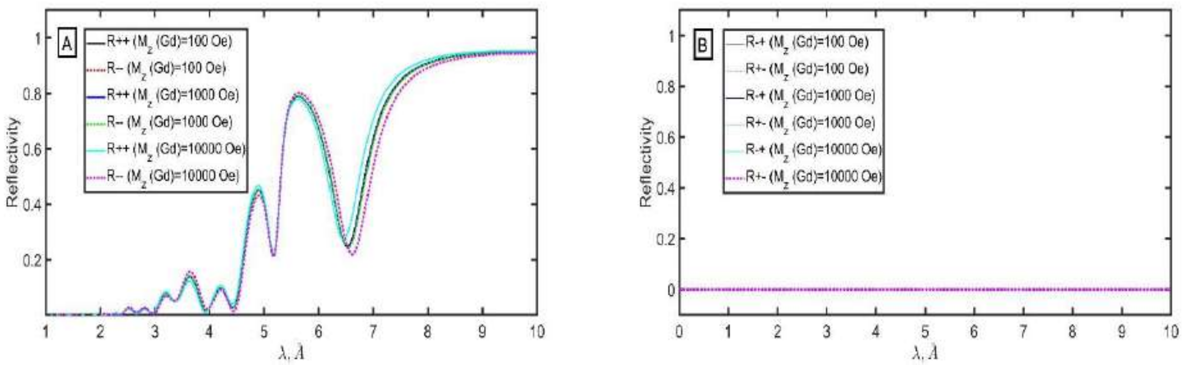

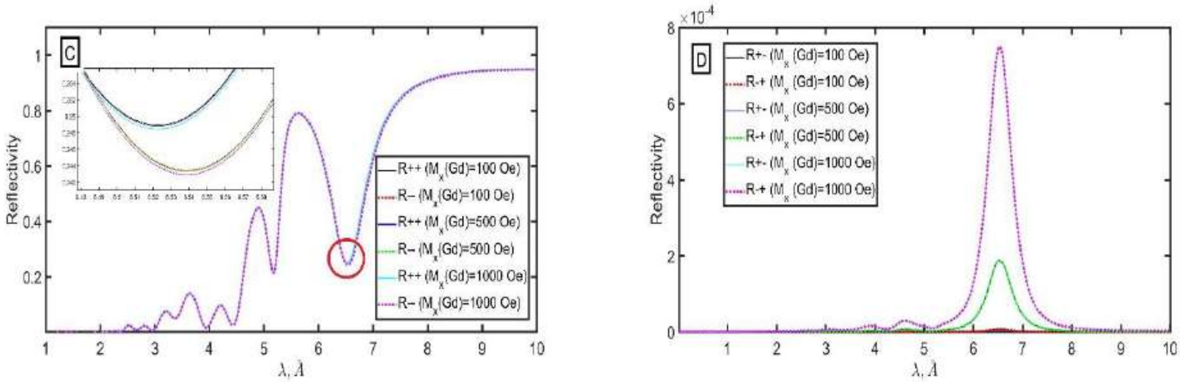

Fig. 5: Neutron reflectivity of the proposed structure at collinear (A & B) and non-collinear (C & D) magnetization of Gd layer.

Fig. 6 shows the calculated neutron reflectivity of the proposed structure versus thicknesses of Gd layer varying from 3 nm to 12 nm at zero magnetization. In Fig. 6(A), increasing the thickness of Gd leads to an increase in the absorbance of neutrons, and the reflectivity spectrum decreases. A similar analysis was performed by setting one of the flippers up and the second one down. The measured reflectivity curves (R-+ and R+-) coincide with each other. The solid lines mean the first flipper is off and the second one is on, but the dotted lines mean the first flipper is on and the second one is off.

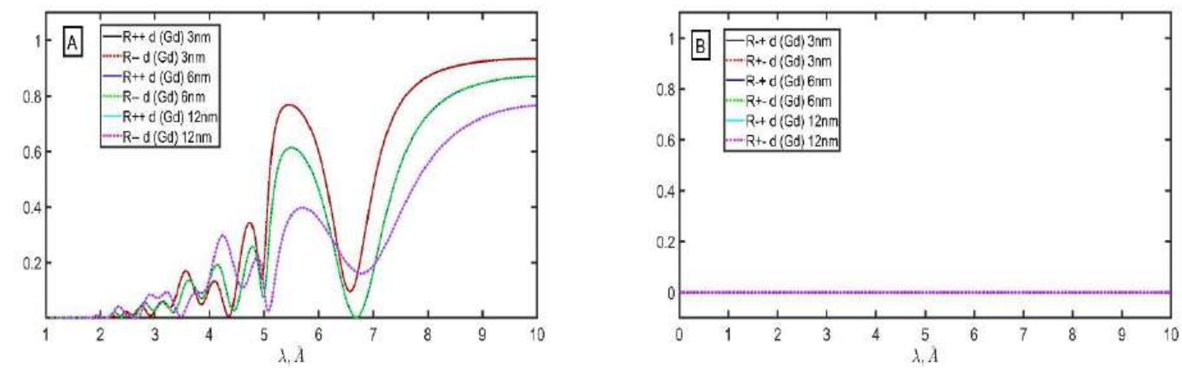

Fig. 6: Neutron reflectivity at different thicknesses of Gd layer at M=0 Oe.

X-ray reflectivities versus grazing angle are calculated using X'Pert reflectivity tool. X-ray reflectivity can give qualitative and quantitative phase analysis of both composite and pure materials. Besides, it provides us with crystal size and preferred orientation. In Fig. 7, because of constructive interference of reflected X-rays from the sample, Bragg peaks are appeared according to Bragg's law:

$$n\lambda = 2d\ sin\theta, \qquad (3)$$

where n, λ, d and θ are the order of interference, wavelength, interplanar spacing, and Bragg angle. By changing the thickness of Gd layer or replacing the Gd layer with Fe, Co, Ni and Dy, Bragg's pattern slightly changed.

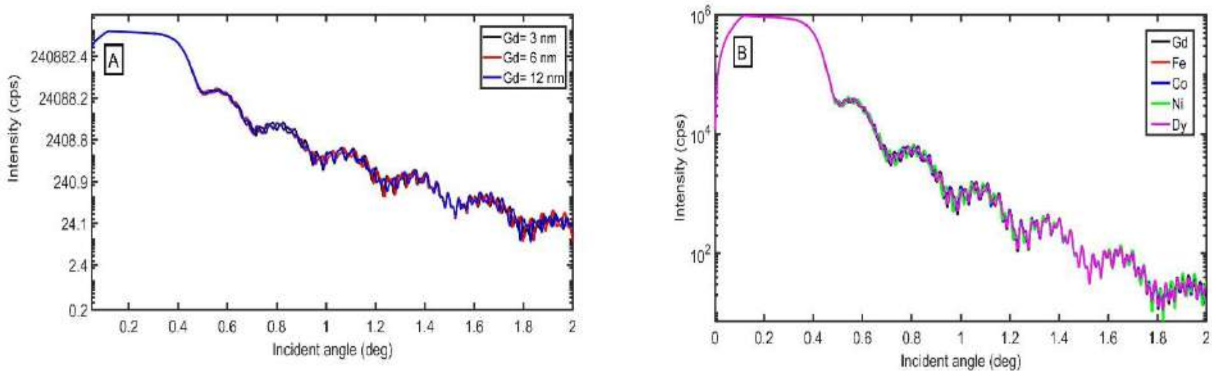

Fig. 7: X-ray reflectivity (A) at different thicknesses of Gd (B) using different ferromagnetic materials at M=0 Oe.

In addition, the observed neutron reflectivities of the proposed structure versus different ferromagnetic materials with scattering length density 8.024 * 10^{-6} /Å^2, 2.265* 10^{-6} /Å^2, 9.408* 10^{-6} /Å^2, and 5.356 * 10^{-6} /Å^2 for Fe, Co, Ni, and Dy, respectively are presented in Fig.8. As clear in Fig. 8(A), other than Gd, at small wavelengths, material with the highest scattering length density records the highest reflectivity at some wavelengths (4.68 nm) but records the lowest reflectivities at other wavelengths (4.10 nm). For wavelengths higher than 5 nm, reflectivities of Fe, Co, Ni, and Dy coincide with each other and record the highest reflectivities. On the other hand, Gd records the lowest reflectivity because it has the highest absorbance. By making the flippers opposed to each other, all reflectivities coincide as clear in Fig. 8(B).

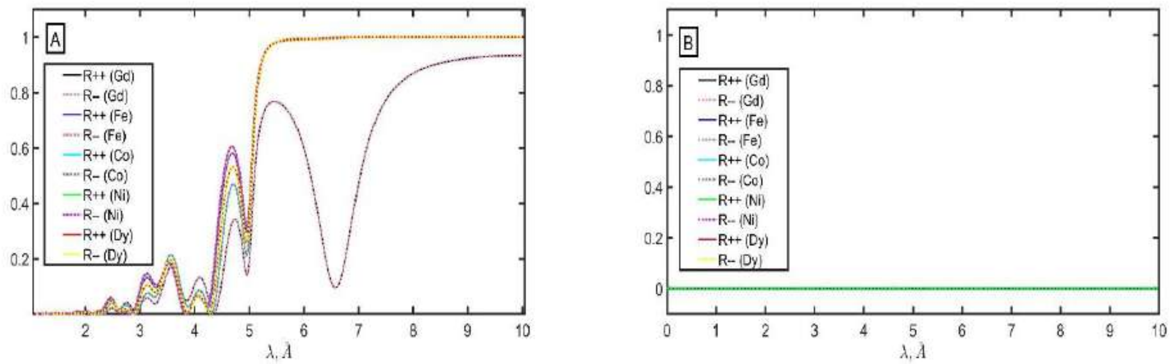

Fig. 8: Neutron reflectivity of different ferromagnetic materials at M=0 Oe.

In Fig. 9(A), neutron reflectivities for different number of unit cells [Nb(25nm) / Gd(3nm)] are calculated. For all Ns, both R++ and R-- behave in the same way. But, at low values of wavelengths, we observe that increasing N resulted in increasing reflectivity (as shown in the inset). This is stemmed from increasing the number of interfaces in the structure. At higher wavelengths, this increase in reflectivity is not noticed. Fig. 9(B) shows the same behavior as Fig. 5(B).

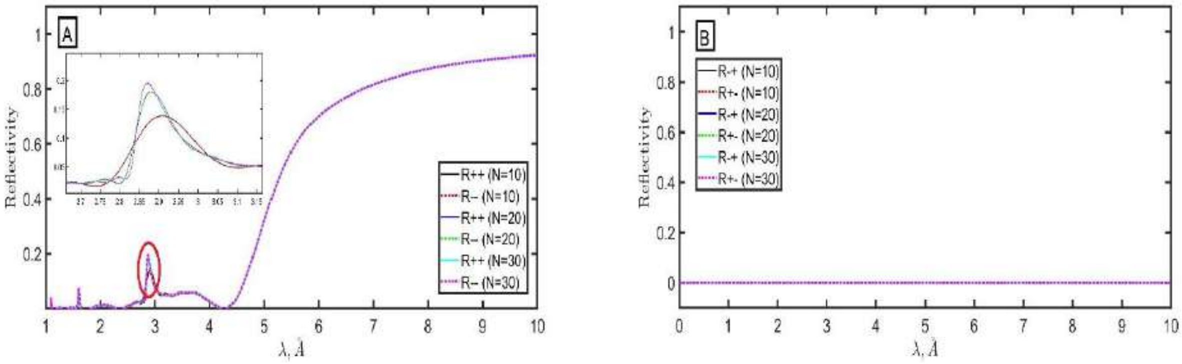

Fig. 9: Neutron reflectivity of different unit cells (N) at M=0 Oe.

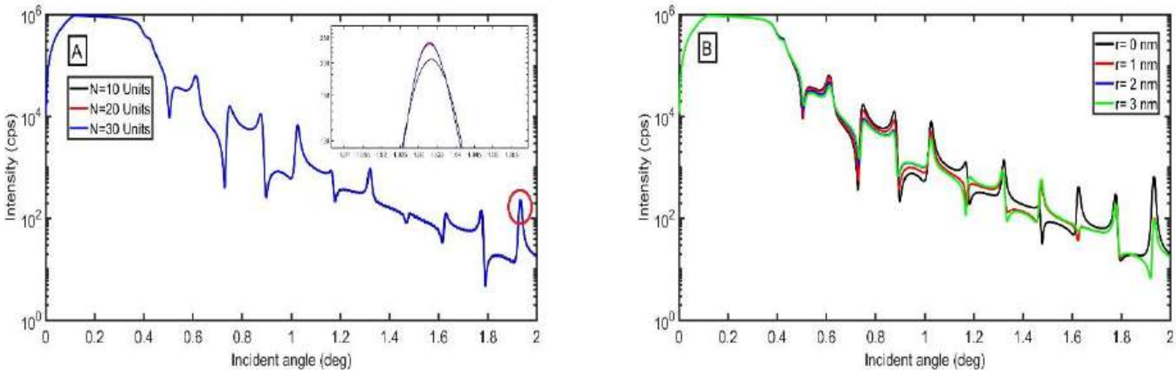

Fig. 10: X-ray reflectivity of different (A) unit cells, (B) roughness at M=0 Oe.

By changing the number of unit cells (N) over a wide range from 10 to 30, the intensity of the reflected x-rays slightly changed. With increasing of N, the number of interfaces increases, and the reflectivity slightly increases, as clear in Fig. 10(A). In Fig. 10(B), the effect of roughness on X-ray reflectivity is cleared. With increasing the roughness of the sample from 0 nm to 3 nm, there is no change at small angles. By increasing the grazing angle, a significant change appears as clear in Fig. 10(B).

Conclusion

The proposed structure consists of Al2O3 / Nb(100nm) / Gd(3nm) / V(70nm) / Nb(15nm). PNR and XRR were used to investigate the magnetization vector and the structural properties of the sample, respectively. After fitting and selecting the optimum conditions, the quality of the fitted data was enhanced and the value of χ^2 decreased to -653.2. Increasing the grazing angle led the reflectivity curves to be shifted to higher values of wavelength. Besides, a significant change in the reflectivity of the sample appeared when the magnetization of the incident neutrons is transformed from collinear to noncollinear state. As a result of increasing the gadolinium thickness, it was noticed that the reflectivity of the sample strongly decreased. Under the effect of changing the type of the magnetic materials, gadolinium showed dissimilar behavior from the other materials. On increasing the roughness of the sample from 0 nm to 3 nm, there was no change found at small angles. While on increasing N, the number of interfaces increased, and the reflectivity slightly increased.

Acknowledgement

We would like to thank Dr. Vladimir Zhaketov for his assistance and his fruitful discussions. Also, we express our deepest gratitude to both the ASRT and JINR committee for giving us this great opportunity to learn, not only academically, but also, on a social and personal level.

References

1. Y. A. Izyumov, Y. N. Proshin, and M. G. Khusainov, "Competition between superconductivity and magnetism in ferromagnet/superconductor heterostructures," Physics-Uspekhi **45**, 109 (2002)

2. A. I. Buzdin, "Proximity effects in superconductor-ferromagnet heterostructures," Reviews of modern physics **77**, 935 (2005)

3. R.-G. Cai and R.-Q. Yang, "Coexistence and competition of ferromagnetism and p-wave superconductivity in holographic model," Physical Review D **91**, 026001 (2015)

4. Y. N. Khaydukov, E. Kravtsov, V. Zhaketov, V. Progliado, G. Kim, Y. V. Nikitenko, T. Keller, V. Ustinov, V. Aksenov, and B. Keimer, "Magnetic proximity effect in Nb/Gd superlattices seen by neutron reflectometry," Phys. Rev. B **99**, 140503 (2019)

5. L. Li, Y. Li, Y. Jin, H. Huang, B. Chen, X. Xu, J. Dai, L. Zhang, X. Yang, and H. Zhai, "Coexistence of superconductivity and ferromagnetism in Sr 0.5 Ce 0.5 FBiS 2," Phys. Rev. B **91**, 014508 (2015)

6. S. Nandi, W. Jin, Y. Xiao, Y. Su, S. Price, D. Shukla, J. Strempfer, H. Jeevan, P. Gegenwart, and T. Brückel, "Coexistence of superconductivity and ferromagnetism in P-doped EuFe 2 As 2," Phys. Rev. B **89**, 014512 (2014)

7. Y. N. Khaydukov, V. Aksenov, Y. V. Nikitenko, K. Zhernenkov, B. Nagy, A. Teichert, R. Steitz, A. Rühm, and L. Bottyán, "Magnetic proximity effects in V/Fe superconductor/ferromagnet single bilayer revealed by waveguide-enhanced polarized neutron reflectometry," J. Supercond. Nov. Magn **24**, 961-968 (2011)

8. C. Majkrzak, K. O'Donovan, and N. Berk, "Polarized neutron reflectometry," in *Neutron Scattering from Magnetic Materials* (Elsevier, 2006), pp. 397-471.

V. Zhaketov